EVOLUTION OF THE KINEMATIC AND THERMAL FIELDS DURING THE DEVELOPMENT OF HURRICANE ELLA (1962)

M. A. ALAKA [1] AND D. T. RUBSAM

National Hurricane Research Laboratory, Environmental Science Services Administration, Miami, Fla.

ABSTRACT

Observations made at different levels by aircraft of the Research Flight Facility (RFF) of the U.S. Weather Bureau, in conjunction with regular synoptic observations from the coastal United States and Bahamas, are utilized in detailed analysis of conditions prevailing during the crucial period immediately before, during, and after Ella (1962) attained hurricane intensity.

It is shown that, in contrast with other hurricanes described in the literature, Ella did not develop under an upper tropospheric anticyclone. Rather, anticyclonic circulation first appeared in the middle troposphere and gradually extended upward while the storm was intensifying into a hurricane. Correspondingly, the warm-core structure first appeared in the low levels and then spread to the upper troposphere.

1. INTRODUCTION

Hurricanes are known to form in pre-existing tropical disturbances. The disturbances are many, but hurricanes are few. Therefore, some selective processes must operate which determine whether or not intensification into a hurricane will occur.

One of the first steps in understanding the nature of the cyclogenetic processes leading to hurricane formation is an accurate description of the structure of the disturbance and its modification during the critical hours immediately before the hurricane is born. Knowledge of these features would increase our insight into the manner in which the atmosphere forms its hurricanes and is an indispensable requisite for the successful formulation of theoretical and numerical models of hurricane genesis.

Because hurricanes usually form far out at sea, well-documented studies which would reveal details of the changing structure of the incipient storm are not easy to execute. It is however well established that the initial tropical disturbance which eventually spawns a hurricane, initially displays cold-core characteristics, at least on a synoptic scale, while the hurricane itself is a warm-core system. In recent years, starting with the work of Riehl [4], synoptic evidence has accumulated to the effect that a necessary though insufficient link in the chain of processes leading to hurricane formation is the prior super-position of an upper tropospheric anticyclone over the low-level disturbance. Transformation from cold-core to warm-core regime follows in response to this super-position. Confirmation of this sequence of events was found by Yanai [6] in connection with typhoon Doris (1958) and by Alaka [1] in connection with hurricane Carla (1961).

In marked contrast with these two hurricanes, is Ella (1962), whose formation was attended by a different sequence of events. These will be described in the following pages.

2. BACKGROUND AND DATA

The disturbance from which Ella developed, first came into view on October 8, 1962, as an easterly wave with its axis near the Windward Islands and moving in a west-northwestward direction (fig. 1). By 1200 GMT, on October 14, a closed circulation had developed with a mean sea level pressure of 1010 mb. Twenty-four hours later the central pressure had fallen to 1002 mb. and shortly after, the first flights into the incipient storm were made by aircraft of the Research Flight Facility (RFF) at two levels. RFF flights at different levels were also made on the 16th, 17th, and 19th; a summary of these flights is given in table 1. Observations from these research flights, in conjunction with regular synoptic observations from the east coast of the United States and from the Bahamas, permitted detailed analysis of the wind and temperature fields during the crucial period immediately before, during, and after Ella attained hurricane intensity.

3. COMPUTATIONAL PROCEDURES

Tangential and smoothed radial components of the wind were used to compute the fields of horizontal velocity divergence ($\nabla_2 \cdot \mathbf{V}$) and vorticity ($\zeta$). This was done by finite differences on a circular grid (fig. 2) centered on the surface position of the disturbance. The following relations were used:

$$\zeta = \frac{v}{r} + \frac{\partial v}{\partial r} + \frac{\partial u}{r \partial \theta} \tag{1}$$

[1] Present address: Techniques Development Laboratory, Weather Bureau, Environmental Science Services Administration, Washington, D.C.

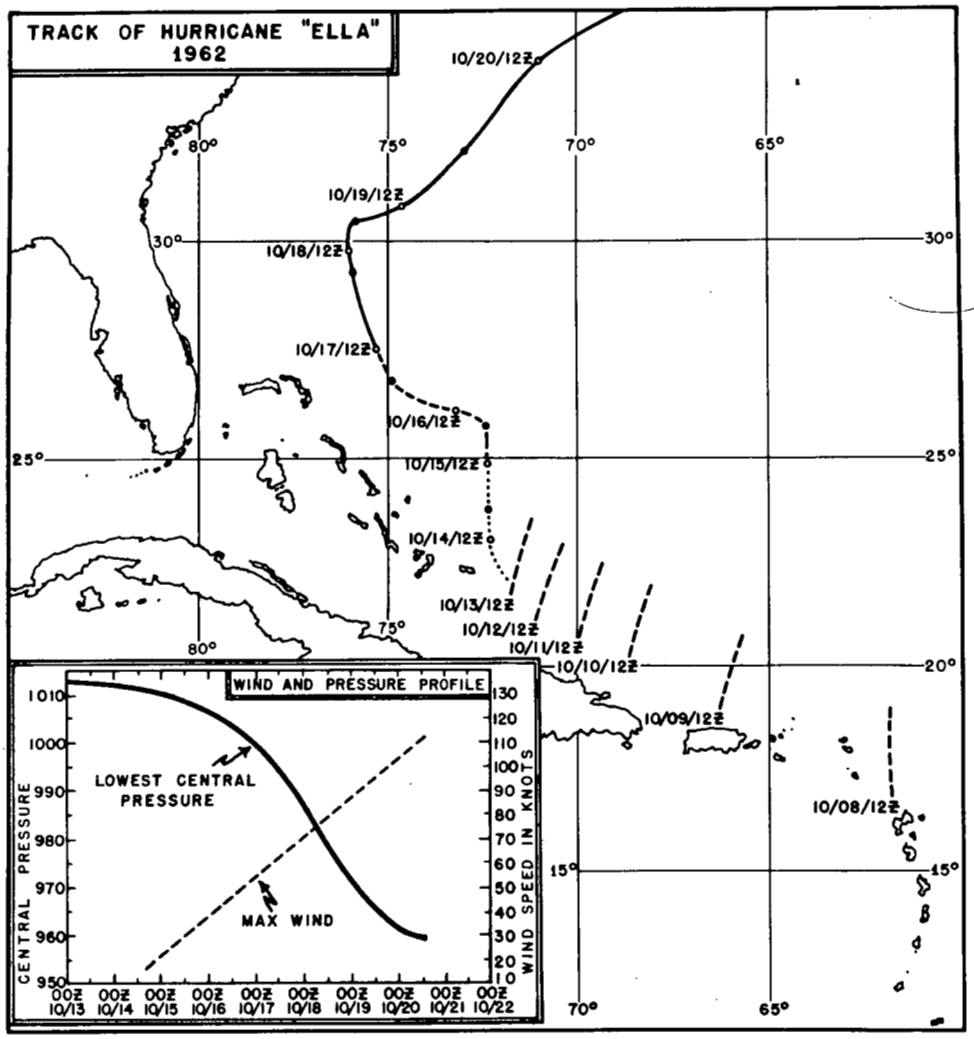

FIGURE 1.—Successive positions of easterly wave from which Ella formed and track of the disturbance in tropical storm and hurricane stages. Inset shows time profiles of mean sea level minimum pressure and maximum wind.

$$\nabla_2 \cdot \mathbf{V} = \frac{u}{r} + \frac{\partial u}{\partial r} - \frac{\partial v}{r \partial \theta} \tag{2}$$

In the above equations, v is the counterclockwise tangential component of the wind, u the outward radial component, r the distance from the center of the grid and θ the azimuth angle measured clockwise. To bring out more clearly the major features in each field the following 9-point smoothing procedure was used. If $\overline{H}_{r,c}$ denotes the smoothed value of $H_{r,c}$ then

$$\overline{H}_{r,c} = \tfrac{1}{16}[4H_{r,c} + 2(H_{r,c+1} + H_{r,c-1} + H_{r+1,c} + H_{r-1,c}) + H_{r+1,c+1} + H_{r+1,c-1} + H_{r-1,c+1} + H_{r-1,c-1}] \tag{3}$$

On the 17th, data at the three flight levels were used to construct vertical profiles of divergence. From these, vertical velocities were computed along two sections across the center of the storm from the following relation:

$$\frac{\partial}{\partial z}(\rho w) + \rho \nabla_2 \cdot \mathbf{V} = 0 \tag{4}$$

If integration is carried between two pressure surfaces p_0 and p_h, such that $p_0 > p_h$, the vertical velocity (w_h) at the latter surface is

$$w_h = \frac{\rho_0}{\rho_h} w_0 - \frac{\overline{\nabla_2 \cdot \mathbf{V}}}{\rho_h g}(p_0 - p_h) \tag{5}$$

where

w_0 = vertical velocity at p_0

ρ_0, ρ_h = density at p_0 and p_h respectively

$\overline{\nabla_2 \cdot \mathbf{V}}$ = mean horizontal velocity divergence between p_0 and p_h

g = acceleration due to gravity.

For mass compensation, care was taken to ensure that the vertical profiles of divergence satisfied the relation

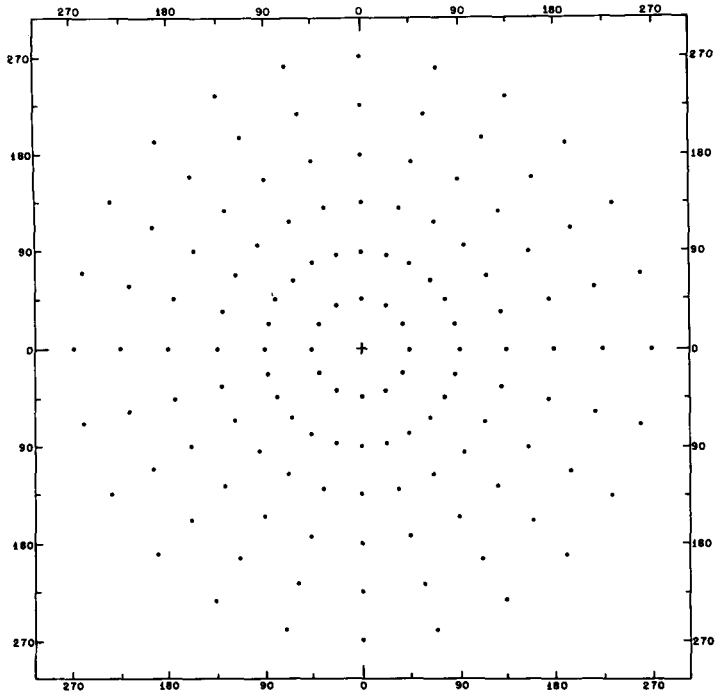

FIGURE 2.—Grid used in the computation of vorticity and divergence.

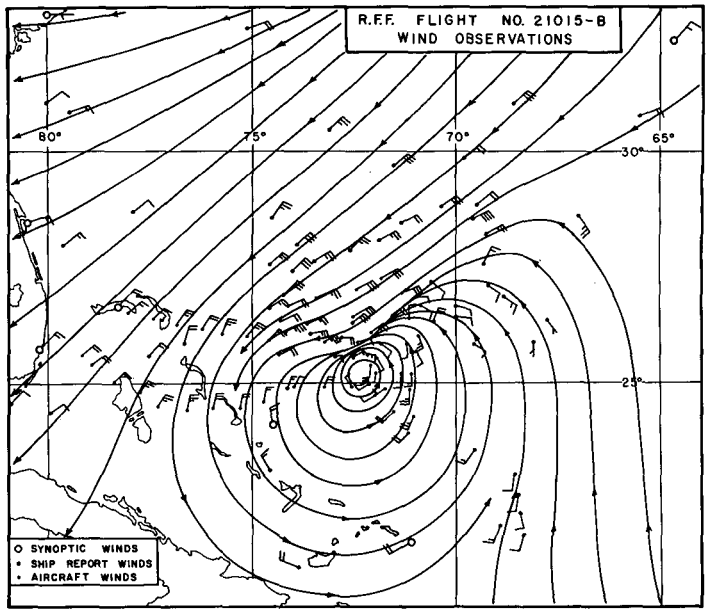

FIGURE 3.—Wind field composited from RFF observations made from 1650–0015 GMT at heights between 2,140 and 2,740 ft. (Flight No. 21015–B), from ship observations and from 1800 GMT synoptic reports on October 15, 1962.

$$\int_{p_0}^{p_T} \nabla_2 \cdot \mathbf{V} dp = 0 \tag{6}$$

where p_0 is the surface pressure and p_T the pressure at the top of the storm which was taken to be 100 mb.

4. THE TROPICAL STORM STAGE

The low-level flight on the 15th (Flight No. 21015–B) made two penetrations into the center of the storm. The first, at 1850 GMT showed a well-defined eye. The eye was, however, found ill-defined on a second penetration at 2125 GMT. Obviously the disturbance was in the process of organizing itself but had already reached tropical storm intensity, a maximum wind of 42 kt. being recorded by the aircraft at 2,500 ft. about 110 mi. north of the center. The minimum mean sea level pressure was 1002 mb. Figure 3 shows the low-level wind field, constructed from flight data, ship reports, and 1800 GMT synoptic reports on October 15. Note the region of strong confluence in the northeast sector.

Figure 4 shows the temperature field, analyzed from observations referred to a standard level of 3,240 ft., and plotted at 10-min. intervals along the path of Flight No. 21015–B. The center of the storm remained almost stationary during the flight, so that the analysis gives a fairly good picture of the temperature field in the storm area. The center is seen to be situated within a strip of high temperature, with the highest temperature of 21° C. (not shown in fig. 4) recorded inside the eye.

The upper flow, revealed by observations made at about the same time by another RFF plane flying at an altitude of about 43,000 ft., is given in figure 5. There is strong difluence downstream from the surface position of the storm but there is no indication, at this level, of any anticyclone. Temperature observations referred to 40,870 ft. (fig. 6) show the storm position at some distance from the highest temperature.

On the 16th, the situation was basically similar in the upper troposphere (figs. 7 and 8), although the storm

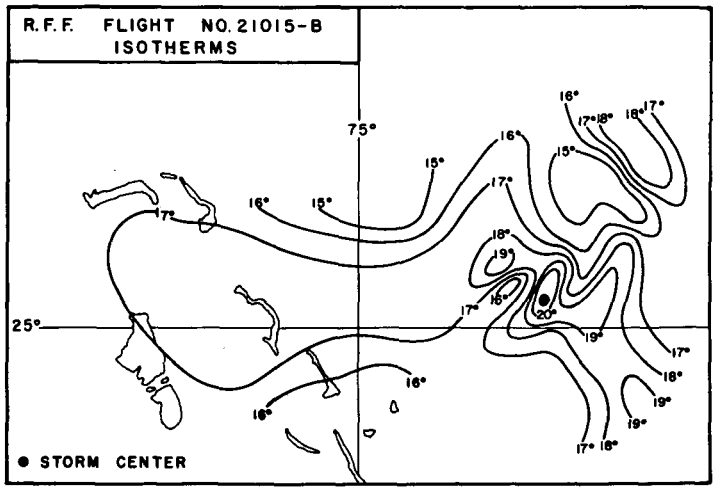

FIGURE 4.—Temperature field (°C.) from RFF observations referred to 3,240 ft., made from 1650 to 0115 GMT on October 15, 1962, by RFF Flight No. 21015–B. The analysis was made from a plot of observations at 10-min. intervals along the flight path.

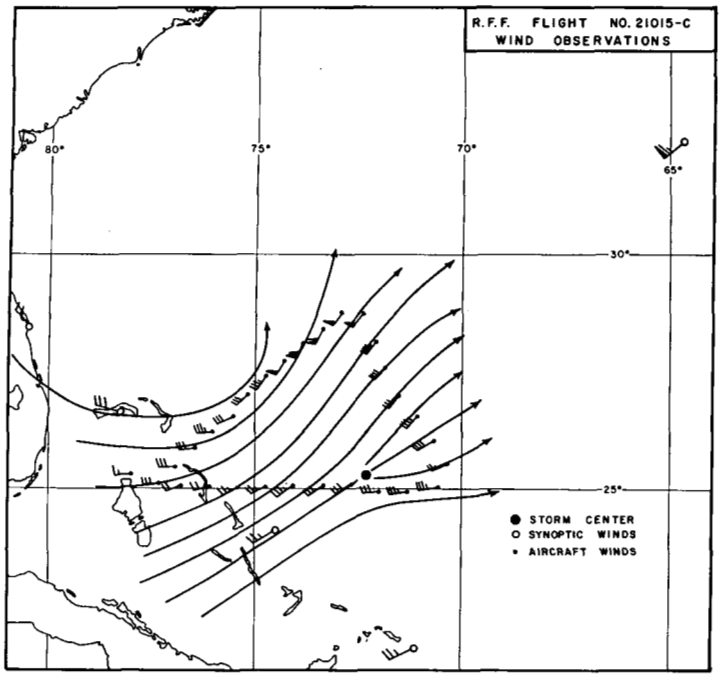

FIGURE 5.—Wind field as depicted by RFF Flight No. 21015–C (see table 1) and 200-mb. rawin synoptic observations at 1800 GMT, October 15, 1962.

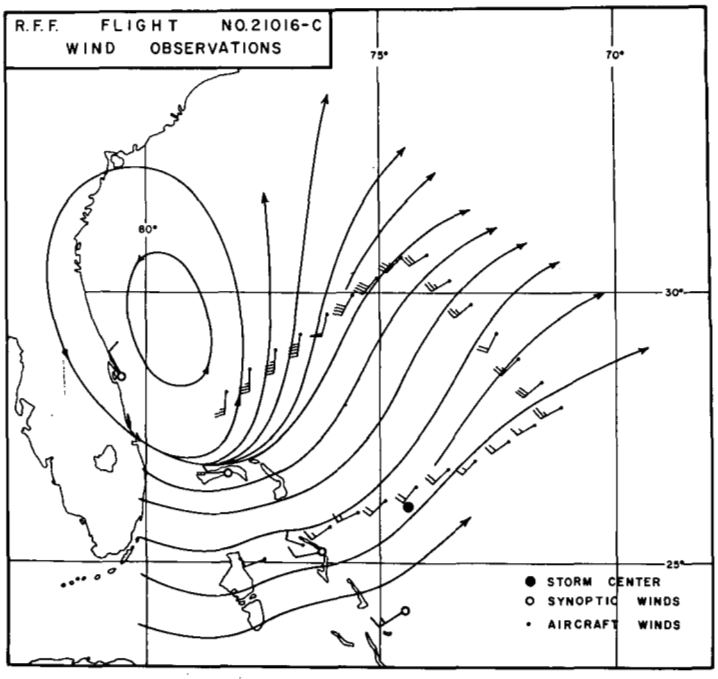

FIGURE 7.—Wind field as depicted by RFF Flight No. 21016–C (see table 1) and 43,000-ft. rawin synoptic observations at 1800 GMT, October 16, 1962.

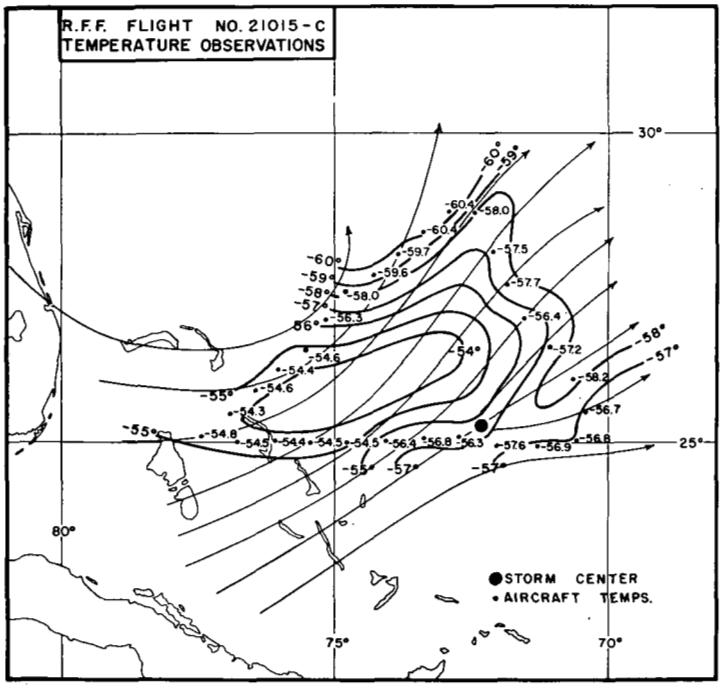

FIGURE 6.—Thick lines: isotherms (°C.) drawn from observations made by RFF Flight No. 21015–C (see table 1). Thin lines: streamlines reproduced from figure 5.

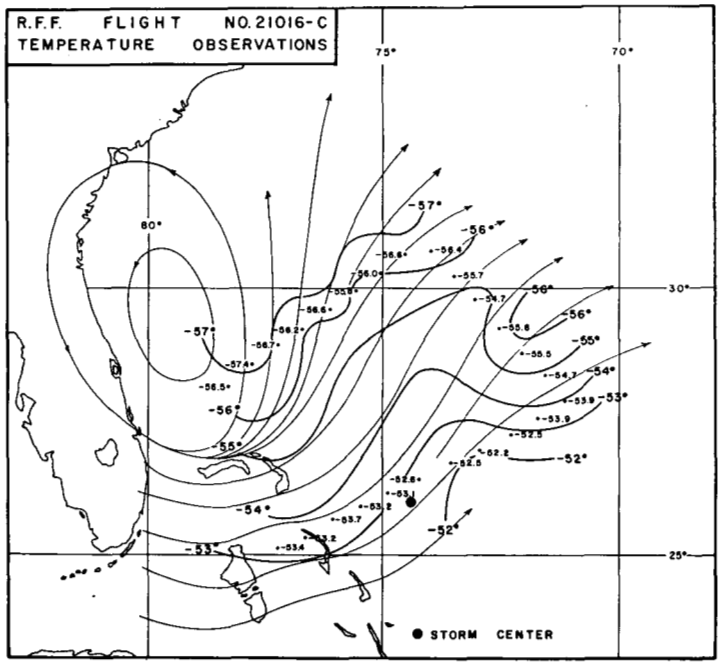

FIGURE 8.—Thick lines: isotherms (°C.) drawn from observations made by RFF Flight 21016–C (see table 1). Thin lines: streamlines reproduced from figure 7.

TABLE 1.—*Research Flight Facility flights into hurricane Ella (1962)*

Date	Flight	Time (GMT)	Height (ft.)	Reference Level (ft.)
October 15, 1962	21015-B	1650-0115	2,140- 2,740	3,240
15	21015-C	1720-1945	39,751-43,010	40,870
16	21016-A	1725-2350	7,953- 9,207	8,090
16	21016-C	1730-1935	40,387-43,979	40,870
17	21017-A	1640-0050	12,877-14,983	13,800
17	21017-B	1550-0030	2,140- 2,708	3,240
17	21017-C	1920-2125	40,501-44,675	40,870
19	21019-A	1100-2120	12,585-14,017	13,800
19	21019-B	1000-2100	1,669- 4,082	3,240
19	21019-C	1225-1440	37,128-45,751	40,870

continued to deepen. The lowest mean sea level pressure was estimated at 994 mb. The maximum wind measured by RFF Flight No. 21016–A (see table 1), flying at about 8,000 ft., was 60 kt. about 60 n. mi. northwest of the center. At this level the storm showed a warm core (fig. 9).

The lower and upper fields of vorticity and divergence during this period are shown in figures 10 to 13. On the 15th, both fields show remarkable asymmetry with respect to the center of the storm. Of particular interest is the field of divergence which in the lower levels (fig. 11a) shows a predominantly convergent flow northeast of the center and predominantly divergent flow to the southwest. In the upper troposphere (fig. 11b) the reverse is true. From continuity, one may conclude that at this stage there was rising motion only in the northeast half of the circulation while in the southwest [2] there was descending motion.

On the 16th, the circulation shows greater organization especially in the low levels (figs. 12a and 13a) where strong fields of cyclonic vorticity and convergence almost surround the center. A somewhat less marked tendency to symmetry is also in evidence in the upper troposphere (figs. 12b and 13b).

5. THE WARMING STAGE

The northwestward movement of the storm brought it into a position where some interesting information may be gleaned about its structure from the neighboring coastal and insular synoptic network. Figure 14 shows the wind field at various levels at 1800 GMT which is about the time of the upper-level RFF Flight No. 21016–C. At 20,000 ft., the low-level cyclonic circulation is still in evidence. The 25,000-ft. level is one of transition. At 30,000 ft., there is a hint of anticyclonic circulation around the storm which becomes more distinct at 35,000 ft. The pattern changes to that shown in figure 7 at about 38,000 ft.

Thus, between the low-level cyclonic circulation and the wave pattern in the upper troposphere, there was a layer, roughly between 30,000 and 38,000 ft. in which the circulation was anticyclonic. Six hours later (fig. 15) the anticyclonic circulation had extended to 40,000 ft. but not to 45,000 ft. The warming thus appears to have propagated upward from the low levels in marked contrast with the findings of Yanai [6] in connection with hurricane Doris (1958) in which the heating first took place in the upper levels and then spread downward. The suddenness with which the wind direction shifts with height above 400 mb. is revealed by figure 16 which represents a time section of the flow at Grand Bahama Island which at 1800 GMT on the 16th, was about 180 mi. from the center of the storm.

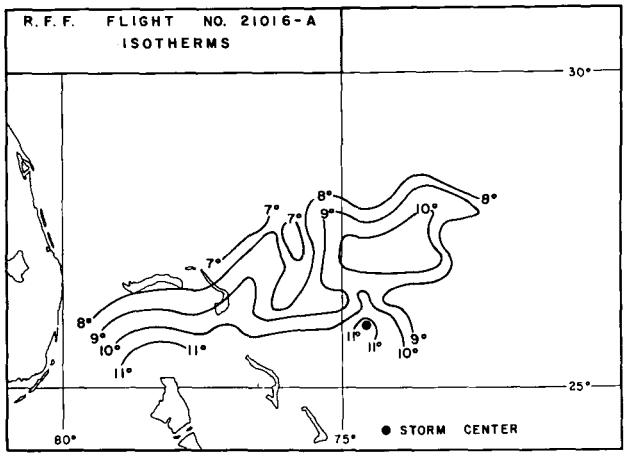

FIGURE 9.—Temperature field (°C.) from observed during RFF Flight No. 21016–A, referred to 8,090 ft.

6. THE NASCENT AND DEVELOPING HURRICANE

Ella was officially proclaimed to have reached hurricane force at about noon on October 17 (Dunn and Staff [2]). Figure 17 shows the wind field in the upper troposphere as depicted by RFF observations made a few hours later. A dramatic change has occurred since the last high-level flight about 24 hr. earlier. Instead of the wave pattern, we have an elongated envelope containing cyclonic eddies one of which coincides with the surface position of Ella. For the first time, there is a hint of a closed anticyclone to the northwest of the storm center.

Upper-air outflow from the central region is clearly discernible and occurs in regions of strong divergence (fig. 18c). In the lower levels (figs. 18a, b) convergent flow almost completely surrounds the center. Particularly noticeable is the similarity between the fields of divergence and convergence at 900 and 600 mb. Figure 19 shows two cross sections of the vertical motion across the center of the storm. In contrast with conditions about two days earlier, there is now ascending motion in all sectors of the storm.

The vorticity field shows a further increase in symmetry at the lower levels (figs. 20a, b) but not in the higher levels (fig. 20c). At this time the center of the storm was situated a little south of 30° N. where the value of the Coriolis parameter is about 7×10^{-5} sec.$^{-1}$. Thus figure

[2] *It is not possible to relate this asymmetry with movement of the storm since, as mentioned earlier, it was almost stationary at this time.*

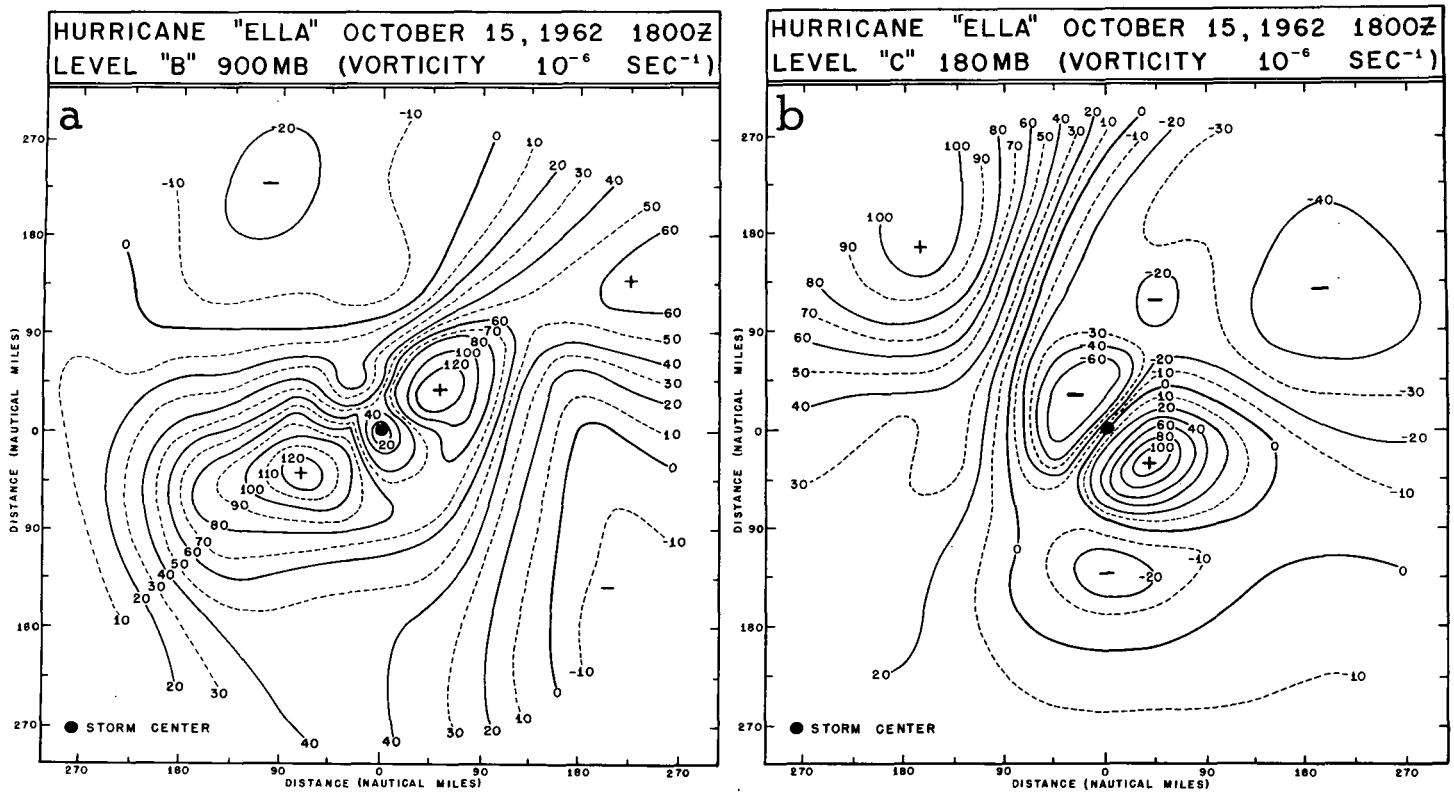

FIGURE 10.—Fields of vorticity computed, from winds observed by: (a) RFF Flight 21015–B; (b) RFF Flight 21015–C (see table 1).

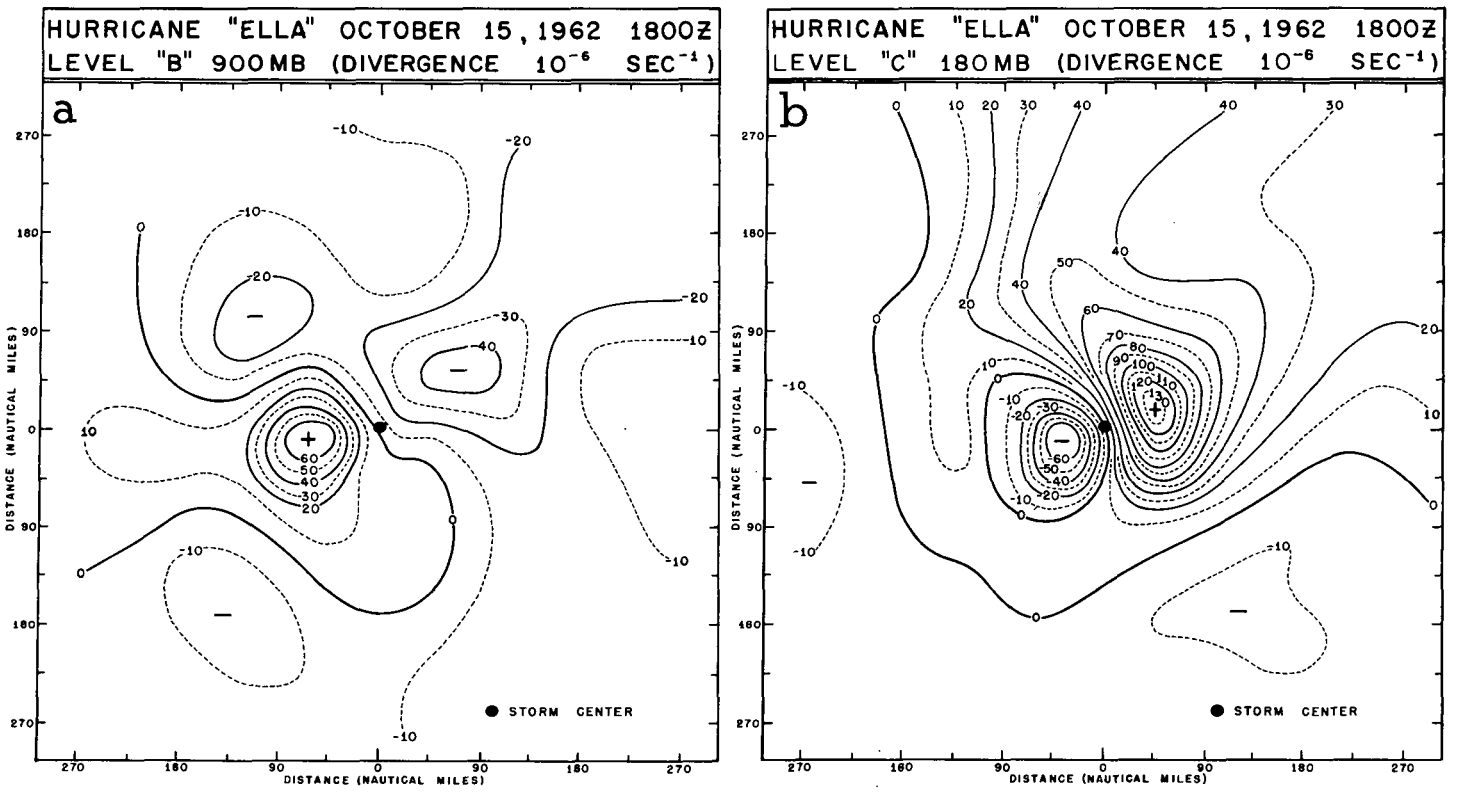

FIGURE 11.—Fields of divergence computed from wind observed by: (a) RFF Flight 21015–B; (b) RFF Flight 21015–C.

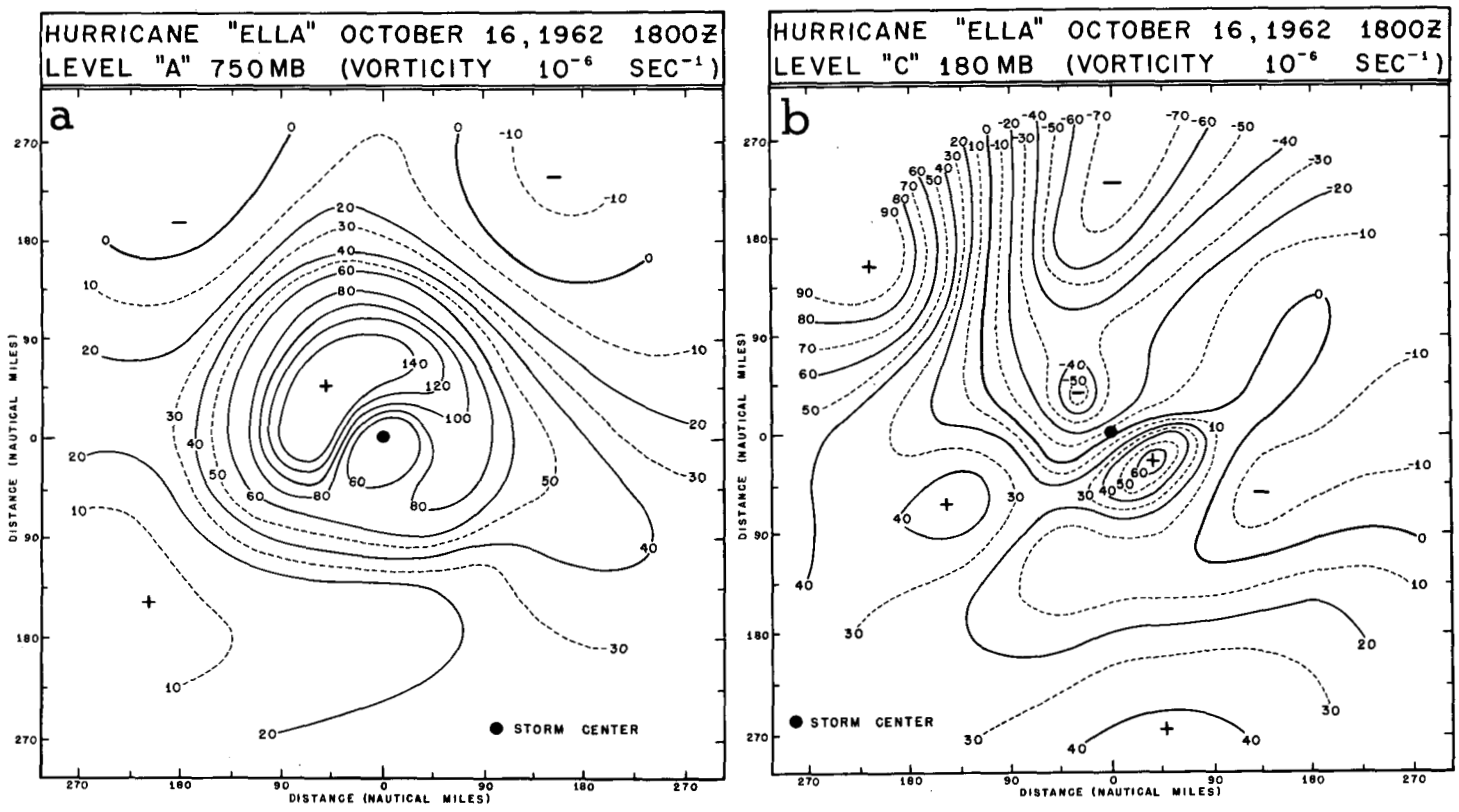

FIGURE 12.—Fields of vorticity computed from: (a) Flight 21016–A; (b) Flight 21016–C.

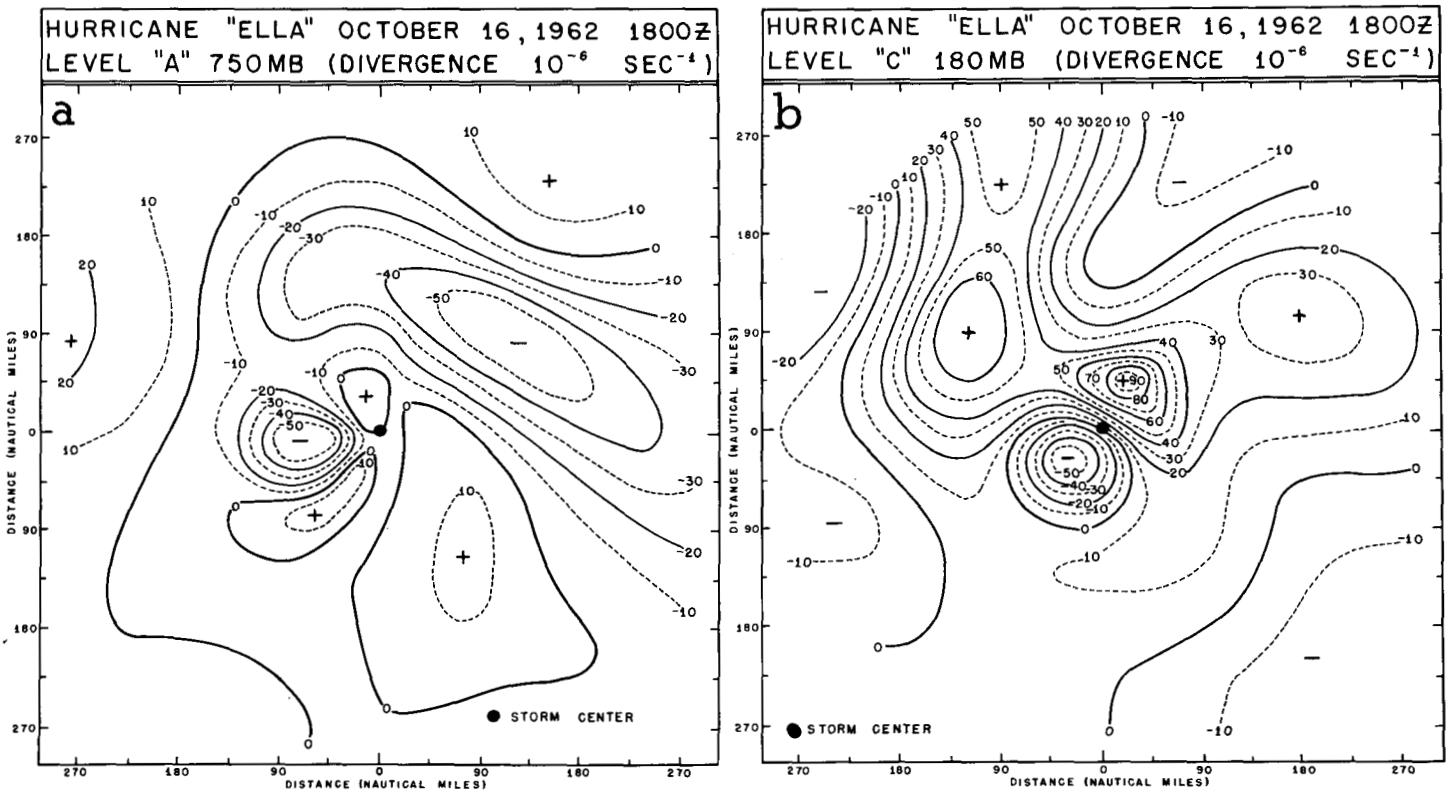

FIGURE 13.—Fields of divergence computed from: (a) Flight 21016–A; (b) Flight 21016–C.

789-641 O—65——4

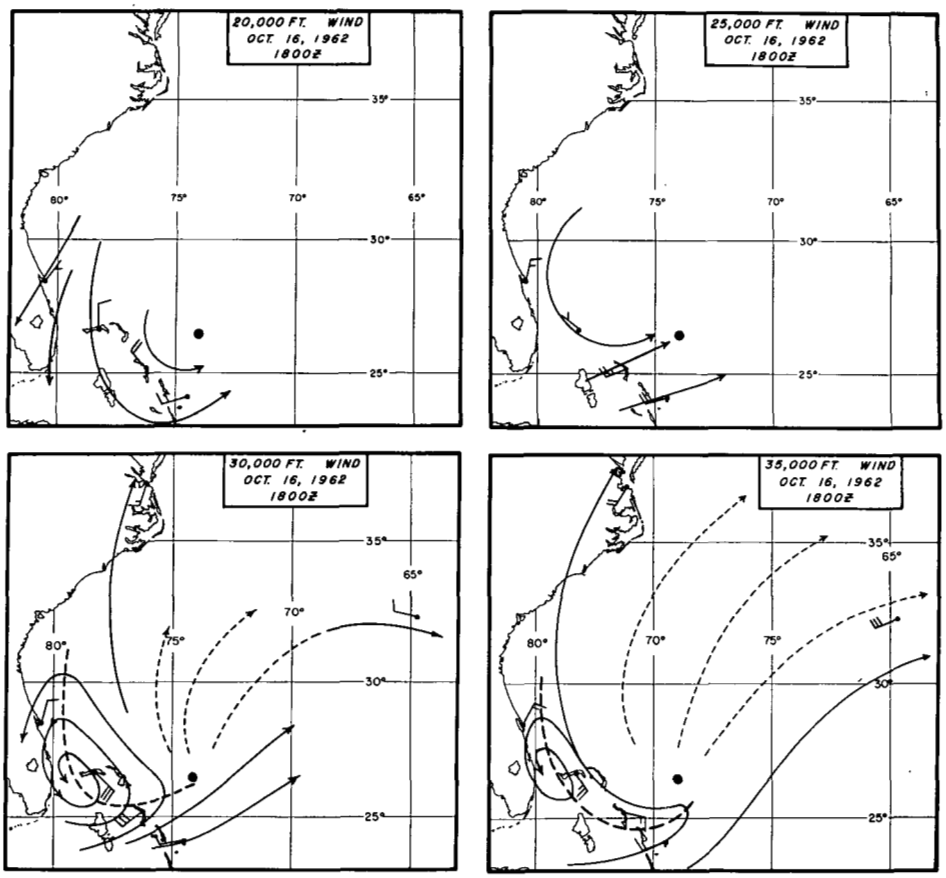

FIGURE 14.—Wind field at various levels in the vicinity of Ella at 1800 GMT October 16, 1962.

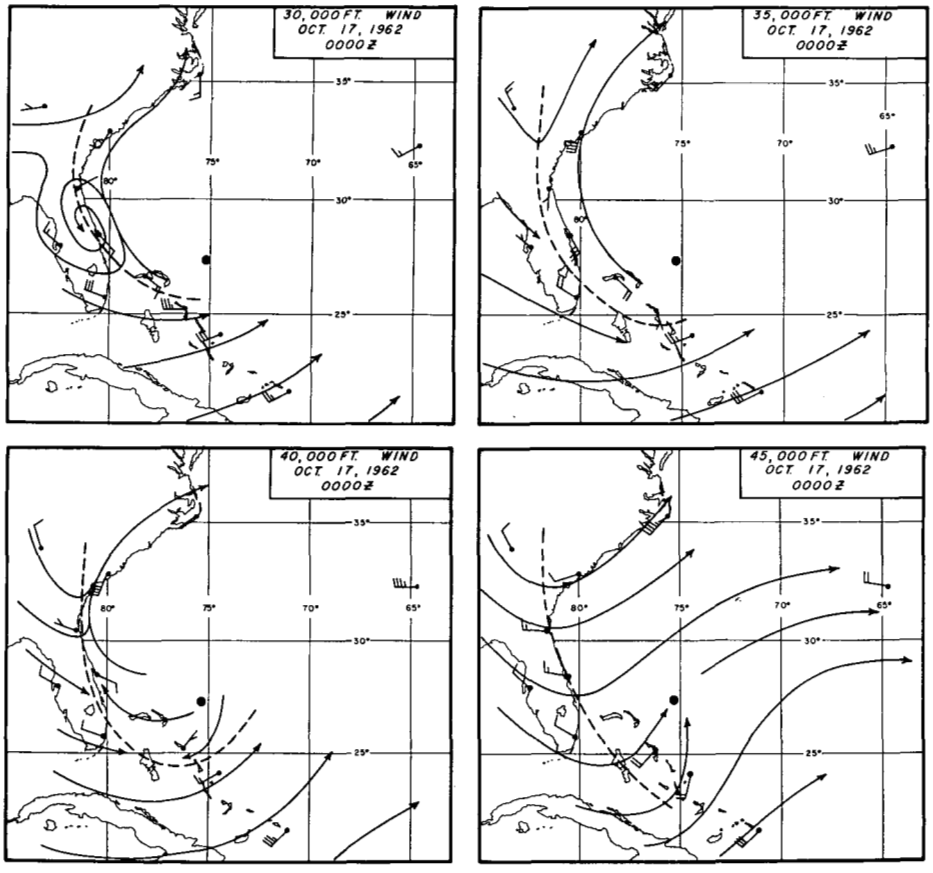

FIGURE 15.—Wind field at various levels in the vicinity of Ella at 0000 GMT October 17, 1962.

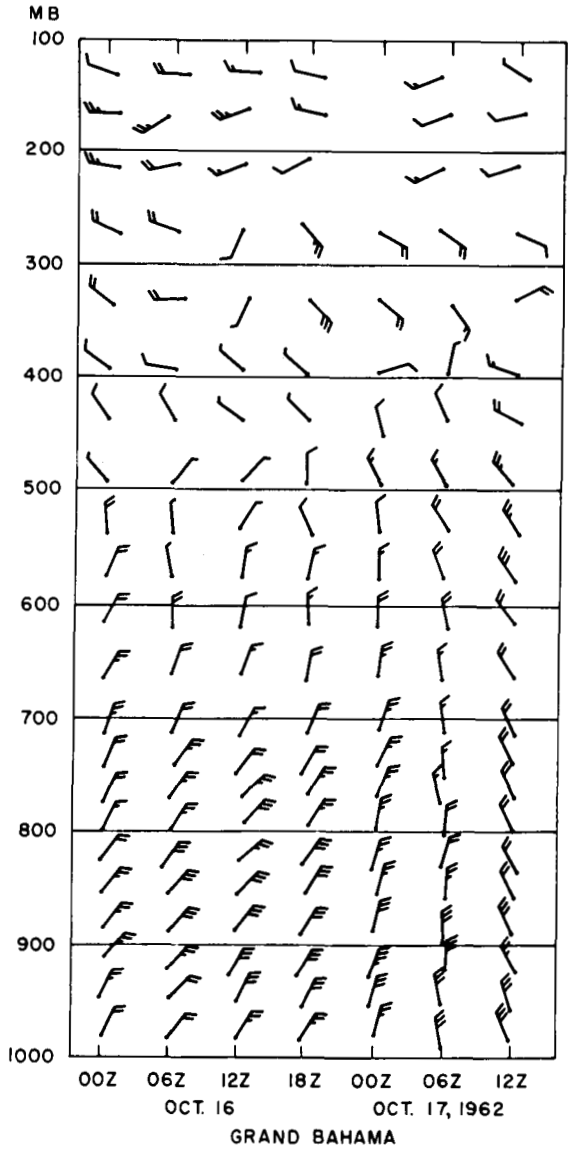

FIGURE 16.—Time section of the wind at Grand Bahama Island.

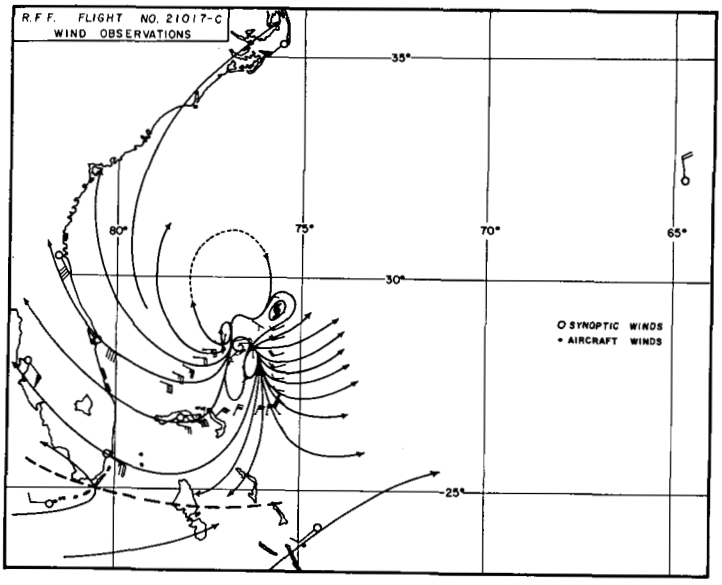

FIGURE 17.—Wind field as depicted by RFF Flight No. 21017–C (table 1) and mean layer rawins (37,000–43,000 ft.) at 0000 GMT October 18, 1962.

20c indicates that a sizable area to the west and southwest of the center was characterized by negative absolute vorticity which is associated with inertial instability.

The temperature field has also changed considerably. In the lower levels (fig. 21a) there is now a strong warm core. An inchoate warm core is also in evidence in the upper troposphere (fig. 21b), but the temperature gradient is still very weak, the difference between the highest and lowest observed being of the order of 3° C.

It was only about two days later, when Ella had become a full-fledged hurricane with 90-kt. winds and mean sea level central pressure of 970 mb., that a clear, warm core with strong temperature gradient became evident in the upper troposphere (fig. 22). By that time divergent flow had completely surrounded the central core of the storm (fig. 23), and the area of negative absolute vorticity ($\zeta < -7 \times 10^{-5}$) had greatly expanded (fig. 24).

7. CONCLUSION

We have seen that, in contrast with other hurricanes described in the literature, Ella did not develop under an upper-tropospheric anticyclone. Rather, the anticyclonic circulation first appeared in the middle troposphere and gradually extended upward with the deepening of the storm. It was thus a result, or at most, a concomitant rather than a requisite of initial deepening. It is believed that Ella may be typical of a class of late-season Atlantic hurricanes which develop in the higher latitudes of the Tropics and are more rarely observed than such typical tropical Atlantic hurricanes as Carla (1961). Cases bearing some similarity to Ella have however been reported in the Australian region by MacRae [3] and Wilkie [5].

ACKNOWLEDGMENTS

The authors wish to express their thanks to George E. Fisher for programing the computations of divergence and vorticity, and to Robert Carrodus and Charles True for assistance with the illustrations.

REFERENCES

1. M. A. Alaka, "Instability Aspects of Hurricane Genesis," *National Hurricane Research Project Report* No. 64, U.S. Weather Bureau, 1963, 23 pp.
2. G. E. Dunn and Staff, "The Hurricane Season of 1962," *Monthly Weather Review*, vol. 91, No. 3, Mar. 1963, pp. 199–207.
3. J. N. MacRae, "The Formation and Development of Tropical

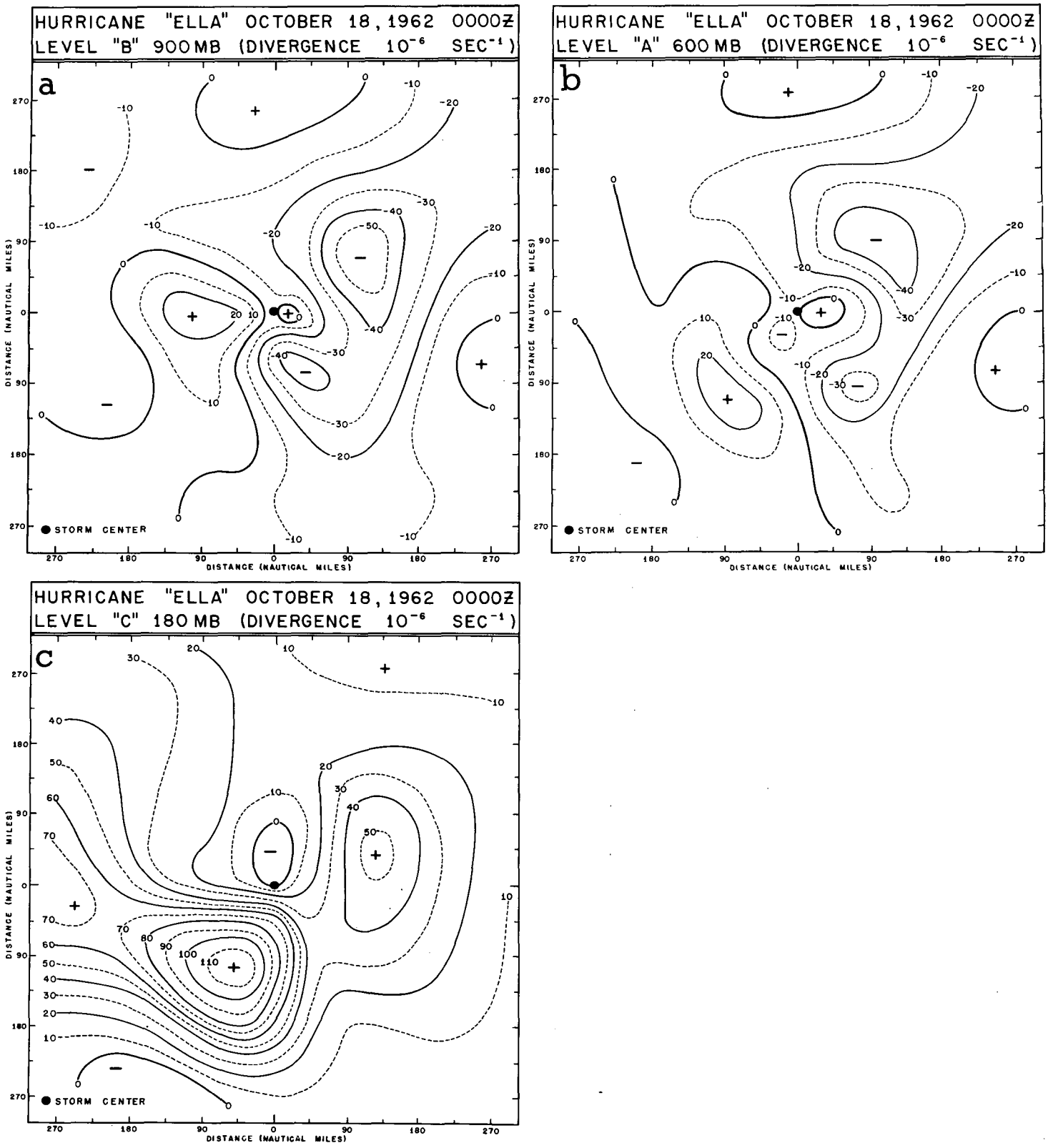

FIGURE 18.—Fields of divergence from RFF Flights: (a) 21017–B; (b) 21017–A; (c) 21017–C.

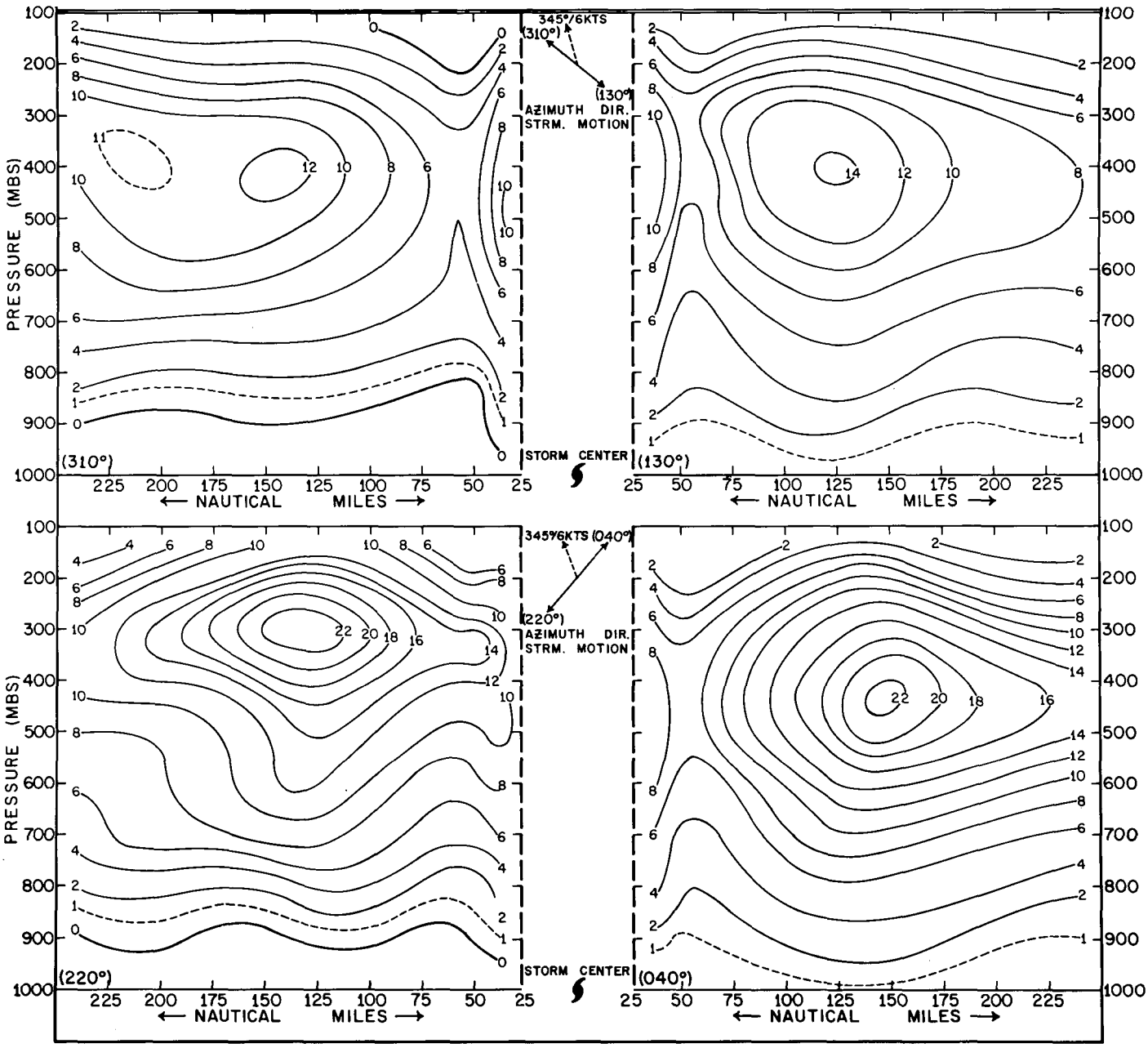

FIGURE 19.—Vertical velocity (cm. sec. $^{-1}$) across hurricane Ella computed from divergence fields at three levels determined from observations by RFF Flights 21017-A, 21017-B, and 21017-C.

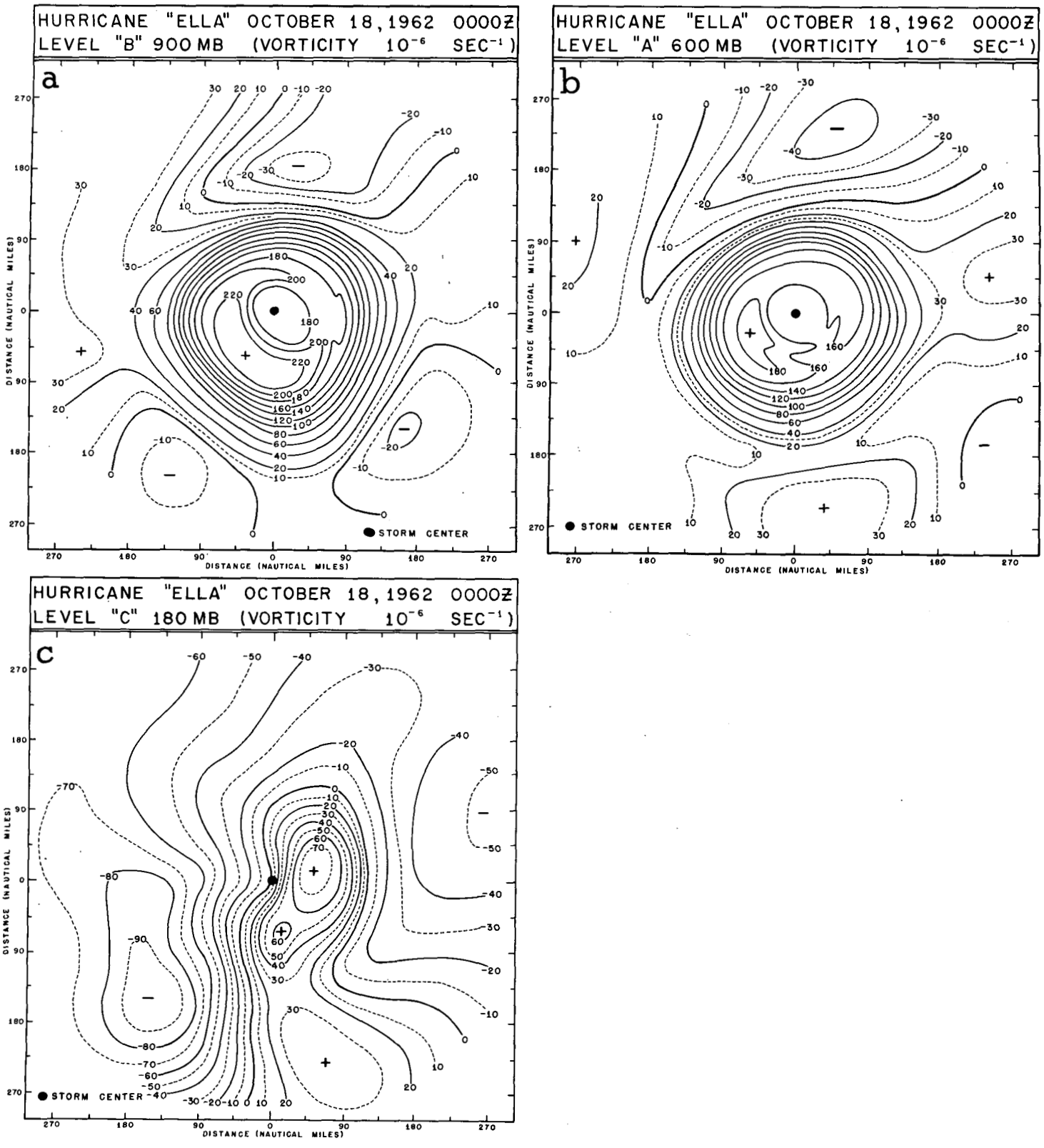

FIGURE 20.—Fields of vorticity from RFF Flights: (a) 21017–B; (b) 21017–A; (c) 21017–C.

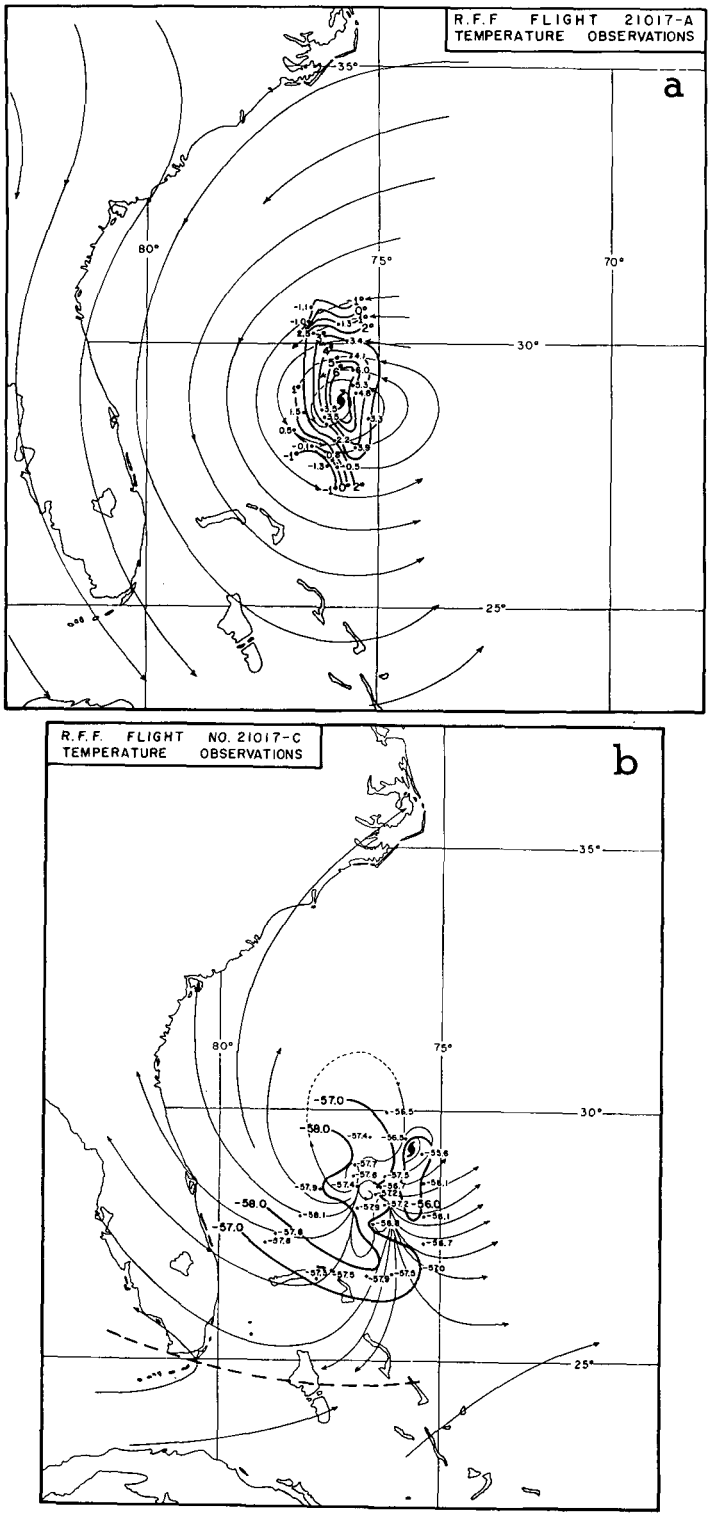

FIGURE 21.—Isotherms (thick lines) in °C. drawn from observations made by RFF Flights: (a) 21017–A; (b) 21017–C.

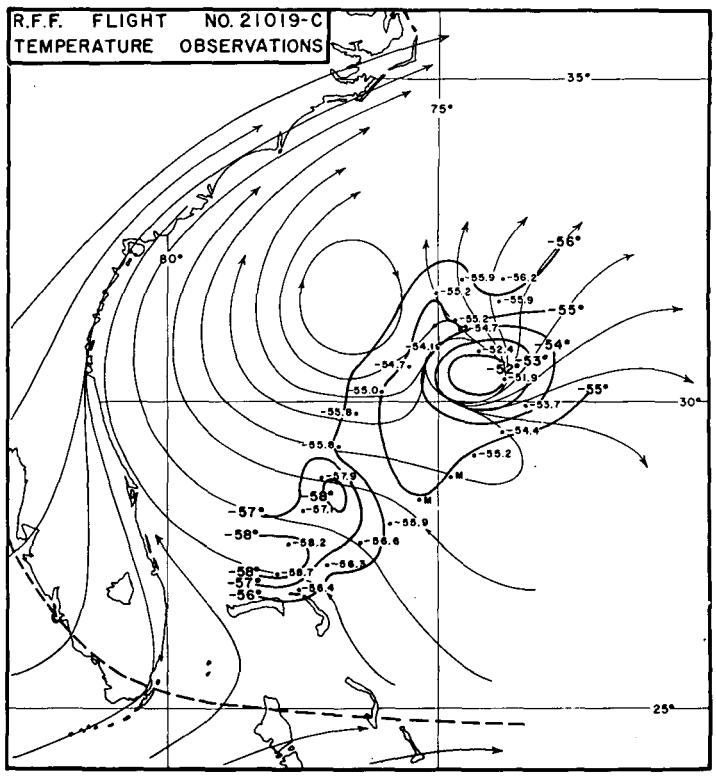

FIGURE 22.—Thick lines: Isotherms drawn from observations by RFF Flight No. 21019–C (table 1). Thin lines: Streamlines drawn from wind observations made during the same flight (not shown) and from 43,000-ft. rawin observations at 1200 GMT, October 19, 1962.

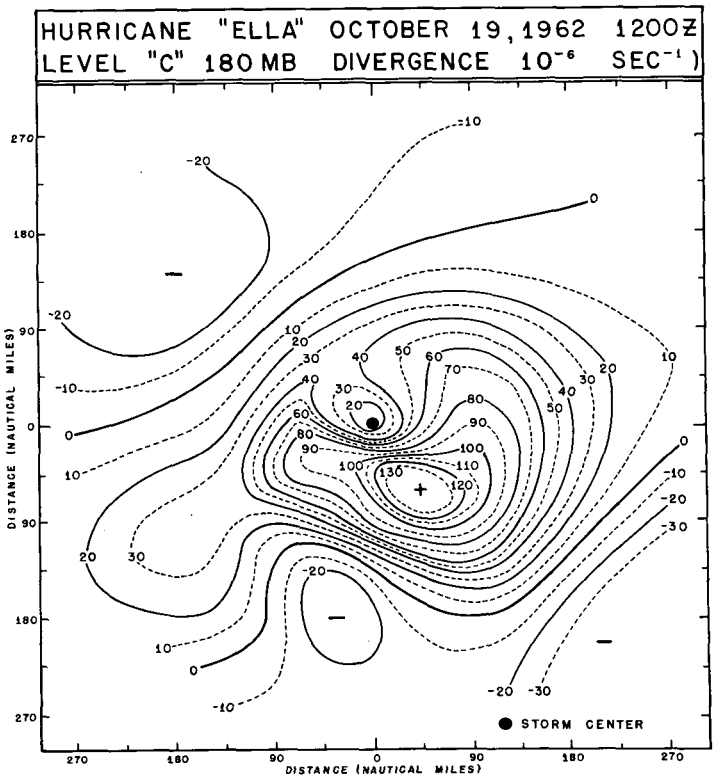

FIGURE 23.—Divergence computed from Flight 21019–C.

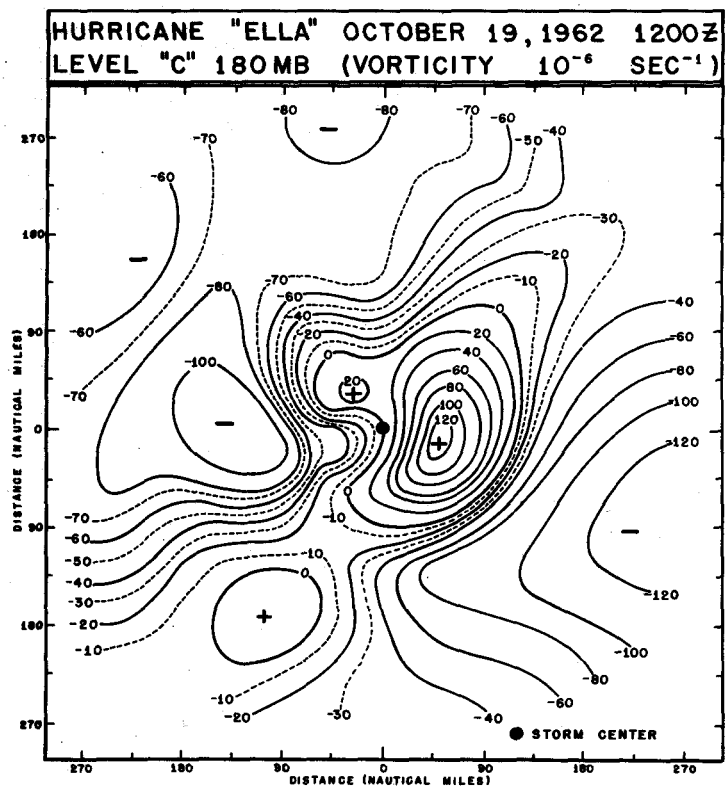

FIGURE 24.—Vorticity computed from Flight 21019-C.

Cyclones During the 1955–56 Season in Australia," *Proceedings of the Tropical Cyclone Symposium, Brisbane, December 1956*, Issued by Director of Meteorology, Melbourne, Dec. 1956.

4. H. Riehl, "On the Formation of Typhoons," *Journal of Meteorology*, vol. 5, No. 6, Dec. 1948, pp. 247–268.
5. W. R. Wilkie, "Evaluation of Methods of Forecasting Development and Movement of Cyclones in the Northeast Australia Region," *Proceedings of the Symposium on Tropical Meteorology, Rotorua, New Zealand, 5–13, November 1963*, New Zealand Meteorological Service, Wellington, 1964.
6. M. Yanai, "A Detailed Analysis of Typhoon Formation," *Journal of the Meteorological Society of Japan*, Ser. 2, vol. 39, No. 4, Aug. 1961, pp. 187–214.

[*Received May 28, 1965; revised August 25, 1965*]

CORRECTION

Vol. 93, No. 9, Sept. 1965, pp. 540 and 541, tables 1, 3, and 4:
The units of E should be labeled kilojoules cm.$^{-2}$ instead of joules m.$^{-2}$